Effect of drying methods of Al_2O_3-GO powder mixture on the properties and microstructure of sintered composites obtained by spark plasma sintering

Pavel Fokin[1,*], *Pavel* Peretyagin[1], and *Anton* Smirnov[1]

[1]Moscow State University of Technology "STANKIN", Vadkovskij per. 1, Moscow, 101472, Russian Federation

Abstract. Well-dispersed alumina ceramic-graphene oxide (GO) powder mixtures were fabricated using a colloidal processing route and three drying techniques were applied: in vacuum, spray and freeze dryers. Dense composites were obtained via spark plasma sintering, the technique reducing GO to graphene in situ during the sintering process. The mechanical properties of the sintered composites were investigated. The composites obtained by spray drying have shown the fracture toughness of 4.5 ± 0.4 MPa·$m^{1/2}$, and hardness of 18.4 ± 0.8 GPa with an extremely high dispersion of graphene within the ceramic matrix.

1 Introduction

The design of ceramic composite materials comprising two or more phases where at least one shows dimensions in the nanometre range has gained increased attention during the past few years.

Alumina (Al_2O_3) is the most widely used oxide ceramic material. Its applications are widespread, and include spark plugs, tap washers, pump seals, electronic substrates, grinding media, abrasion resistant tiles, cutting tools, bioceramics, body armour, laboratory ware and wear parts for the textile and paper industries [1]. However, the greatest drawback of ceramics is their low fracture toughness.

Graphene seems as a suitable filler for fracture toughness improvement in ceramic composites. The addition of graphene as a second phase with its unique combination of thermal [2], electrical [3] and mechanical properties [4] improves the performance of the bulk composite.

Graphene oxide (GO) is graphite that has been oxidized to intersperse the carbon layers with oxygen molecules, and then reduced, to separate the carbon layers completely into individual or few layer graphene. In addition, GO has been considered widely as a prominent precursor and a starting material for the synthesis of this processable material. GO is of great interest due to its low cost, easy access, and widespread ability to convert to graphene. Scalability is also a much desired feature.

Therefore, in order to improve mechanical properties, especially fracture toughness, GO was added to the corresponding ceramic matrix [5].

Spark Plasma Sintering (SPS) was chosen as rapid consolidation technique [6-9] that allowed reducing the sintering temperature and avoiding undesirable grain growth of alumina.

Moreover, the characteristics of powder mixtures were influenced by the different drying methods and, consequently, sintered samples properties were depend on them as well. However, the aspects of drying methods have been poorly studied yet.

The purpose of the present study was to obtain dense Al_2O_3-GO ceramic composites with enhanced mechanical properties and to describe the influence of different drying methods on the quality of a powder mixtures and, consequently, on sintered materials.

2 Materials and characterization

2.1 Raw materials

Commercially available α-alumina nanosized powder (Plasmotherm, Moscow, Russia) with a chemical purity of 99.5% and average particle size of 180 nm was used as a matrix material. Graphene oxide was synthesized by using a modified Hummer's method through oxidation of commercial graphite powder with a chemical purity of 99.9% [10].

2.2 Powder processing and sintering

Suspension of Al_2O_3-0.5 vol.% GO was prepared using a colloidal method [5]. Al_2O_3 powder were added to 100 mL of water at a pH 10, previously fixed by adding NH_4OH. The Al_2O_3 powder was dispersed by stirring for 30 min. Then, the appropriate amount of the graphene oxide suspension was dropwise to the ceramic powder

* Corresponding author: pashafokin94@mail.ru

dispersions. The mixed powder suspensions were stirred for 1 h.

Slurry of powder was prepared using distilled water as liquid media via dry ball mill (ML-1, Kaluga, Russia), containing alumina balls, in polyethylene containers at 150 rpm during 24 h.

After homogenization mixture was dried using three different equipments: Mini Spray Dryer B-290 (BÜCHI Labortechnik AG, Flawil, Switzerland) spray dryer equipped with a nozzle, in a vacuum drying oven VO 200 (Memmert GmbH Co. KG, Schwabach, Germany) and FreeZone 2.5 freeze-drying system (LabConco, Kansas, MO, USA).

The spray dryer was composed of a cylindrical chamber with an 800 mm internal diameter and 564 mm height, followed by a conical chamber of 564 mm high with a 60° angle. The powder was separated off the stream of hot air in a cyclone and collected directly into a glass pot. Operational conditions of the spray dryer were set as follows: feed flow rate: 20 mL/min; air flow rate: 130 m^3/h; inlet air temperature 200 ± 2°C; outlet air temperature, varies with inlet temperature.

Meanwhle, in freeze-drying system the suspension was dried at the collector temperature of -50 ± 2°C. Furthermore, the shell temperature and the chamber pressure were kept at +23 ± 2◦C and 0.02 ± 0.01 mbar, respectively, during the entire process.

These methods make it is possible to obtain a "ready-to-sinter powder" without sieving.

On the other hand, after drying in vacuum oven at the 90 ± 1°C the resulting powder was ground in an agate mortar and subsequently passed through a 75 μm sieve in order to avoid agglomeration.

Powder densification was performed by SPS KCE-FCT-H-HP-D25-SD (FCT Systeme GmbH, Rauenstein, Germany) at a maximum temperature of 1000-1400°C (increments of 100°C), reached under vacuum at a heating rate of 100°C/min, and an applied pressure of 80 MPa. The sintered specimens had diameters of 20 mm and thicknesses of 4 mm. For comparison purposes Al_2O_3 powders without GO were SPSed following the same sintering cycle.

2.3 Microstructural characterization

The true density of powder was measured using a gas pycnometer AccuPyc II 1340 (Micromeritics, Norcross, USA). The device operation principle involves sample placing into a calibrated chamber filled with helium. To clean the sample surface from water vapors and impurities, one need to start from several helium blowdowns, and after that the analysis itself can be conducted. The gas molecules penetrate the tiniest sample pores. In other words, the sample pushes out the gas volume equal to the volume of the true solid phase only. In case the sample weight was preliminary entered, the device will calculate its density.

Scanning electron microscopy (SEM) characterization was carried out on polished down to 1 μm surfaces by VEGA 3 LMH (SEM Tescan, Brno, Czech Republic).

The density of the sintered samples (ρ) was measured in distilled water using Archimedes' principle and was compared with the theoretical value, calculated according to the rule of mixtures. Raman spectra of as-prepared powders and sintered samples were collected to identify the phase composition. The Raman setup is composed of a laser (DXR^{TM}2 Raman Microscope, Thermo Fisher Scientific, MA, USA) with a wavelength of 532 nm and a laser power of 2.0 mW. The laser beam was focused through an optical microscope's 50× objective lens to a spot size of 50 μm on the studied area (from different spots, at an interval of 200 nm). The accumulation time for each Raman spectrum was about 10 s.

Vickers hardness, *Hv*, was measured on polished surfaces using a Vickers diamond indenter (QNess A10 Microhardness Tester, Salzburg, Austria), applying a load of 1 kg and an indentation time of 10 s. The hardness results were averaged over 10 indentations per specimen.

Fracture toughness (K_{1c}) was determined from Vickers indentations obtained with a load of 10 kg for 10 seconds. The indentation sizes and crack lengths were measured using SEM. The method and formulas for calculating *Hv* and K_{1c} have been reported elsewhere [11].

3 Results and discussion

3.1 Microstructure and Raman characterization

The morphology of Al_2O_3-GO obtained of the scanning electron microscope shown in Fig.1. The powder particles after spray drying (Fig.1A) are spherical and have a narrow size distribution (d_{50} ≈ 20 μm). The microstructure of the powder obtained by freeze-drying (Fig.1B), consists of separate fragments of the layered structure in the form of flakes with an average grain diameter (d_{50} ≈ 400 μm). Particles, dried in a vacuum oven (Fig.1C), have a variety of shapes with an average grain size (d_{50} ≈ 200 μm).

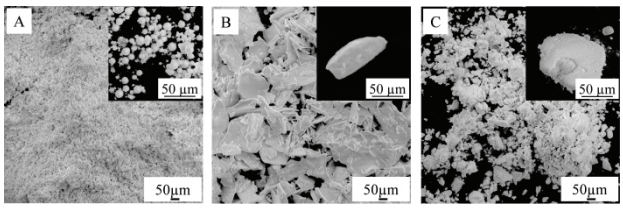

Fig. 1. SEM images of Al_2O_3-GO powder mixtures obtained by spray (a) freeze (b) and vacuum (b) drying.

Raman spectroscopy is an effective method of chemical analysis for studying the composition and structure of substances, allowing to see the thermal recovery of graphene oxide. Fig. 2 a-c shows the Raman spectra that correspond to the mixtures before sintering by SPS; they reveal that all compositions consist of alumina and typical GO peaks. The broad G peak and negligible 2D peak are characteristic of sp^1, sp^2 and sp^3 hybridized carbon–carbon bonds in graphene. The D bands at ~1350 cm^{-1}confirm the lattice distortions. On the other hand, for the specimens sintered at the temperature of 1400ºC (Fig.2 d-f), the intensity of the D peaks decreases while G

peaks increases. This indicates partial heat recovery of graphene oxide, which occurs at a temperature of 1400°C.

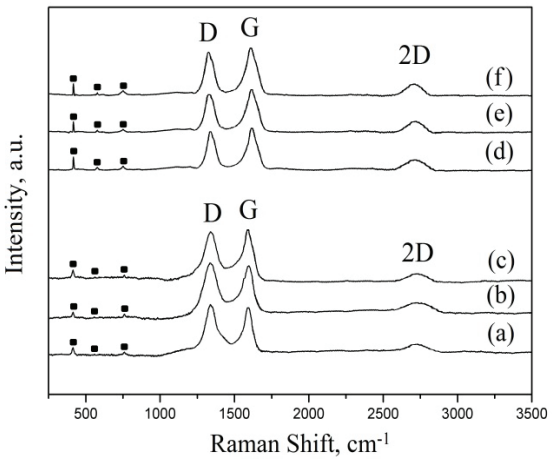

Fig. 2. Raman spectra of as-prepared (a-c) and sintered (d-f) at 1400°C powders Al_2O_3-GO, prepared spray, vacuum and freeze drying, respectively. "▪" label denotes alumina peaks. "D", "G" and "2D" mark GO peaks before and graphene peaks after sintering, respectively.

Figure 3 demonstrates the fracture surface of spray dried and sintered Al_2O_3-GO (Fig. 3B) composite and Al_2O_3 (Fig. 3A) ceramic as well. The average grain size was found to be 3 ± 0.38 μm and 0.8 ± 0.33 μm for Al_2O_3 and Al_2O_3-GO samples, respectively.

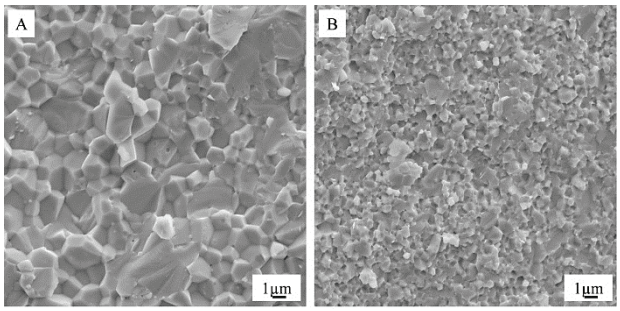

Fig. 3. SEM images showing the representative morphology of Al_2O_3 (A) ceramic and spray dried Al_2O_3-GO (B) ceramic composite fracture surface.

3.2 Mechanical properties

The density of all sintered samples increased with increasing sintering temperature and reach its maximum value (99 – 99.8 % th.) at 1400°C regardless of drying methods applied.

The influence of sintering temperature on hardness and fracture toughness of sintered composites presented on Fig.4 and Fig.5, respectively. Spray dried and sintered at a maximum (1400°C) temperature samples showed the highest value of hardness (≈ 18.4 ± 0.8 GPa). It is explained by the fact that this drying process much faster than other methods and allows to avoid agglomeration of GO in ceramic matrix that often acts as a weaker source for decrease a material's mechanical properties.

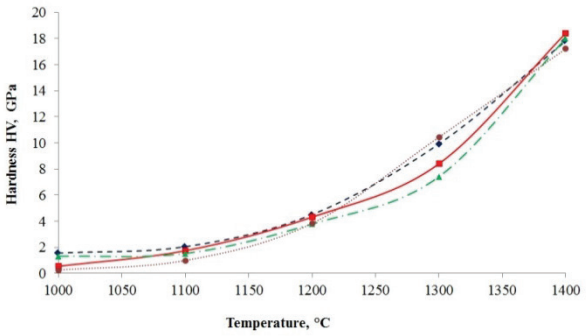

Fig. 4. Influence of sintering temperature on hardness of sintered composites obtained by vacuum (- - -), spray (——), freeze (— · —) drying, and monolithic ceramic Al_2O_3 (···).

Figure 5 shows that the measured fracture toughness of all samples revealed a similar trend, i.e. increased to a maximum value with increasing sintering temperature. The spray dried and sintered Al_2O_3-GO composites exhibited the highest fracture toughness of 4.5 ± 0.4 MPa·m$^{1/2}$ as compared to 3.6 ± 0.4 MPa·m$^{1/2}$ measured for the monolithic ceramic. This value confirms that graphene is well dispersed in the ceramic matrix as well.

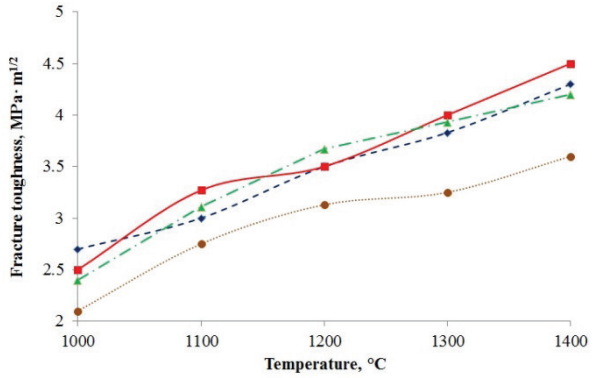

Fig. 5. Influence of sintering temperature on fracture toughness of produced composites obtained by vacuum (- - -), spray (——), freeze (— · —) drying, and monolithic ceramic Al_2O_3 (···).

Fig. 6 shows the Vickers indentation cracks induced on the surfaces of Al_2O_3 ceramic and spray dried Al_2O_3-GO composite. Fig. 6A, corresponding to the Al_2O_3 ceramic, shows a crack path that is mainly comprised of transgranular fractures which, consequently, implies a lower fracture toughness than that of the Al_2O_3-GO spray drying composite. Graphene-reinforced ceramic matrix composites (Fig. 6B) show singly and doubly deflected crack. This effect may be due to the nanodispersed graphene nature. Graphene consists of nanoflakes with a high aspect ratio and could leads to deflection of a crack, additional energy dissipation, and hence, to the enhanced fracture toughness of composites. In addtition, the fracture surface of Al_2O_3-GO composites show a more intricate surface (Fig. 3B) due to a more intergranular fracture and, as a consequence, a higher fracture energy.

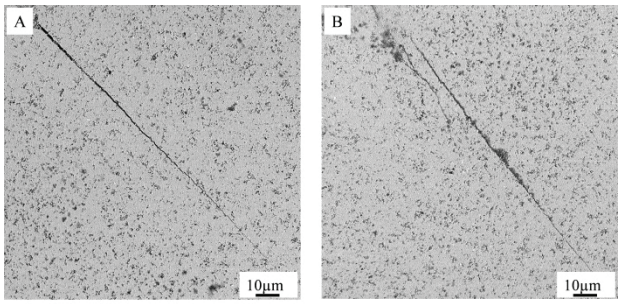

Fig.6. Vickers indentation cracks induced on the surfaces of: Al_2O_3 (A) and Al_2O_3-0.5 vol.% GO (B) samples sintered at 1400°C.

4 Conclusion

Al_2O_3-0.5 vol.% graphene oxide composites have been successfully fabricated by combining a colloidal processing route and Spark Plasma Sintering. Results showed that the addition of low graphene oxide contents to an Al_2O_3 ceramic matrix simultaneously improved fracture toughness and hardness. This mechanical upgrade takes place when small quantities of graphene are homogeneously dispersed in the matrix. The composites containing 0.5 % GO obtained after spray drying method possess the highest fracture toughness (4.5 ± 0.4 MPa·m$^{1/2}$) and hardness (18.4 ± 0.8 GPa) among all studied materials due to obtained a homogeneous and agglomerate-free dispersion of GO inside the alumina matrix. Compared to the Al_2O_3 samples, the samples with graphene oxide in a percentage ratio increased the rate of fracture toughness and hardness by 28% and 6%, respectively. Further scientific research in this area are needed for understanding of impact of graphene/ceramic interfaces on the reinforcing mechanism in composites. The uniform dispersion of graphene and composite's structure retention and control which affect the microstructural evolution during processing might also represent the prospective goal for further research.

Authors would like to thank The Ministry of the Russian Federation supported this work in the frame of Governmental Regulation of the Russian Federation No. 220, 9 April 2010 by contract 14.B25.31.0012, 26 June 2013.

References

1. I.W.M. Brown, W.R. Owers, Curr. Appl. Phys. **4**, 171 (2004)
2. A.A. Balandin, S. Ghosh, W.Z. Bao, I. Calizo, D. Teweldebrhan, F. Miao, C.N. Lau, Nano Lett. **3**, 902 (2008)
3. T. Stauber, N. M. R. Peres, F. Guinea, Phys. Rev. B **76**, 205423 (2007)
4. C. Lee, X. D. Wei, J. W. Kysar, J. Hone, Science **321**, 385 (2008)
5. S. Grigoriev, P. Peretyagin, A. Smirnov, W. Solís, L. A. Díaz, A. Fernández, R. Torrecillas, J. Eur. Ceram. Soc. **37**, 2473 (2017)
6. C. F. Gutiérrez-González, M. Suarez, S. Pozhidaev, S. Rivera, P. Peretyagin, W. Solís, L. A. Díaz, A. Fernandez, R. Torrecillas, J. Eur. Ceram. Soc. **36**, 2149 (2016)
7. N. W. Solís, P. Peretyagin, R. Torrecillas, A. Fernández, J. L. Menéndez, C. Mallada, L. A. Díaz, J. S. Moya, J Electroceram. **38**,119 (2017)
8. S.S. Pozhidaev, A.E. Seleznev, N.W. Solis Pinargote, P. Yu. Peretyagin, Mechanics & Industry **16**, 710 (2015)
9. C.F. Gutierrez-Gonzalez, N.W. Solis Pinargote, S. Agouram, P. Y. Peretyagin, S. Lopez-Esteban, R. Torrecillas, Mechanics & Industry **16**, 703 (2015)
10. W. S. Hummers Jr., R. E. Offeman, J. Am. Chem. Soc. **80**,1339 (1958)
11. A. Smirnov, H. D. Kurland, J. Grabow, F. A. Müller, J. F. Bartolomé, J. Eur. Ceram. Soc. **35**, 2685 (2015)